INL/CON-13-30130
PREPRINT

Modeling the Ductile Brittle Fracture Transition in Reactor Pressure Vessel Steels Using a Cohesive Zone Model Based Approach

International Workshop on Structural Materials for Innovative Nuclear Systems

Pritam Chakraborty
S. Bulent Biner

October 2013

Modeling the Ductile Brittle Fracture Transition in Reactor Pressure Vessel Steels using a Cohesive Zone Model based approach

Pritam Chakraborty *[a] and S. Bulent Biner [a]
[a] Modeling and Simulation Dept., Idaho National Lab.
Idaho Falls, ID 83415-3840, USA
* Corresponding author: pritam.chakraborty@inl.gov

Abstract

Fracture properties of Reactor Pressure Vessel (RPV) steels show large variations with changes in temperature and irradiation levels. Brittle behavior is observed at lower temperatures and/or higher irradiation levels whereas ductile mode of failure is predominant at higher temperatures and/or lower irradiation levels. In addition to such temperature and radiation dependent fracture behavior, significant scatter in fracture toughness has also been observed. As a consequence of such variability in fracture behavior, accurate estimates of fracture properties of RPV steels are of utmost importance for safe and reliable operation of reactor pressure vessels. A cohesive zone based approach is being pursued in the present study where an attempt is made to obtain a unified law capturing both stable crack growth (ductile fracture) and unstable failure (cleavage fracture). The parameters of the constitutive model are dependent on both temperature and failure probability. The effect of irradiation has not been considered in the present study. The use of such a cohesive zone based approach would allow the modeling of explicit crack growth at both stable and unstable regimes of fracture. Also it would provide the possibility to incorporate more physical lower length scale models to predict DBT. Such a multi-scale approach would significantly improve the predictive capabilities of the model, which is still largely empirical.

Introduction

There has been significant effort to model the different failure mechanisms that are active at different temperature regime in RPV steels. At lower temperatures, unstable failure by cleavage fracture is identified as the dominant failure mechanism. This is characterized by slip induced micro-crack formation at carbides and their extension into macroscopic cracks depending on the local deformation state and microstructure. Physics based models have been proposed in (Knott, 1977), (McMahon, 1965) and (Smith, 1966) to explain these mechanisms of cleavage initiation in steel. However these models don't relate cleavage initiation at a microscopic length scale to the fracture toughness. To develop such a correlation, a model has been proposed in (Ritchie, 1973), in which it is assumed that cleavage failure happens when crack tip stress (σ_f) exceeds a critical value over 1 or 2 grain diameters. However this model fails to capture the scatter in fracture toughness associated with cleavage failure. Modifications have been made to this model in (Curry, 1979) in which a critical volume ahead of the crack tip has been considered to explain the scatter in fracture toughness due to cleavage failure. A more rigorous statistical model has been proposed by Beremin (Beremin, 1983) in which a Weibull distribution (Weibull, 1953) is used to relate fracture stress to failure probability at lower and transition temperatures where cleavage fracture is the dominant mechanism. The Weibull parameters are obtained from fracture tests performed at lower temperatures and are assumed to be temperature independent. The temperature dependent variation of fracture toughness is considered by modifying the flow stress of the material. Analytical solutions and FE simulations with hardening plasticity are used to obtain crack-tip stress fields. Though this model has been fairly successful in capturing the scatter in fracture toughness at and near the lower shelf, it requires the modeling of stable crack growth near the transition regime to provide accurate results. Stable crack growth primarily takes place through void nucleation, growth and coalescence. By incorporating ductile damage models proposed by Rousselier (Rousselier, 1987) or Gurson (Gurson, 1977) to simulate stable crack growth prior to unstable failure, improved predictions can be made. In (Tanguy, 2005), DBT using Charpy specimens have been performed using Rousselier model (Rousselier, 1987) in conjunction with Beremin model (Beremin, 1983) to predict onset of cleavage failure. Modifications have been made to the Beremin model by introducing the effect of plastic strain and history of maximum principal stress to evaluate the critical Weibull stress. Irradiation effects have also been considered in their work. DBT of German low alloy pressure vessel steel using CT-specimens have been analyzed in (Samal, 2008) by considering a non-local Rousselier model (Samal, 2008) in conjunction with Beremin model (Beremin, 1983). The non-local model eliminates the mesh-dependency typically observed in local strain-softening models. In addition to the Beremin model, a local stress based model in conjunction with Weibull distribution has also been proposed in (Margolin, 2006) as a cleavage initiation indicator. Though these approaches have been able to capture the fracture toughness variability at and near lower shelf, an improved model consisting of both ductile and cleavage mode of crack growth is necessary to predict the entire DBT region accurately. In addition, the model should have the provision to incorporate more physical lower length scale models as in (Vincent, 2010).

In the present work, a cohesive zone based model has been proposed to analyze DBT in RPV steel. A unified model has been developed which incorporates both ductile damage and cleavage failure mechanisms through temperature and failure probability dependent parameters. The flow strength of the bulk material is varied to obtain the temperature dependent bulk material behavior. It is assumed that without cleavage, the cohesive law follows a traction-separation behavior of ductile-damage as described in (Scheider, 2003). From the known flow-stress evolution at different temperatures separate ductile-damage traction-separation parameters can thus be obtained from a unit cell analysis. However depending on the temperature and failure probability, unloading in the cohesive law due to cleavage can start earlier, and can reduce the fracture toughness of the material. With the use of such a cohesive law, scatter in the fracture toughness with temperature can be successfully obtained. The results from this methodology are compared with experiments and Master Curve reported in (Samal, 2008).

The organization of the paper is as follows: The unified cohesive law to capture ductile damage is described first followed by the calibration process using unit cell analysis to obtain the cohesive law parameters of ductile damage without cleavage failure. The calibration procedure to obtain the cleavage dependent cohesive parameters is described next. Two different temperatures are considered and comparisons are made with experiments. The paper is concluded in the last section.

Unified cohesive zone model

For a material undergoing ductile damage, the underlying traction separation law consists of an initial steady state void growth and coalescence, followed by rapid coalescence and complete loss of strength once a critical void volume fraction is reached. The traction-separation law proposed in (Scheider, 2003) has been used in the present work to represent ductile damage where the traction σ is related to the separation δ by

$$\sigma=\sigma_0\begin{cases} 2\left(\dfrac{\delta}{\delta_e}\right)-\left(\dfrac{\delta}{\delta_e}\right)^2, \text{ when } 0<\delta<\delta_e \\ 1, \text{ when } \delta_e<\delta<\delta_c \\ 2\left(\dfrac{\delta-\delta_c}{\delta_f-\delta_c}\right)^3-3\left(\dfrac{\delta-\delta_c}{\delta_f-\delta_c}\right)^2+1, \text{ when } \delta_c<\delta<\delta_f \end{cases} \quad (1)$$

where σ_0 is the maximum stress and δ_e, δ_c, δ_f are the separation distances when maximum stress is reached, at onset of damage (unloading) and final failure respectively. The global Load-CMOD is nearly insensitive to the shape of the traction-separation law as reported in (Tvergaard, 1992). Hence a constant maximum stress (σ_0) during steady void coalescence has been assumed, as can be seen from Eq. 1. For the unified cohesive law it is assumed that:

(i) For a given flow stress (at a given temperature), the shape of the traction separation law is fixed by ductile damage;

(ii) Depending on temperature and failure probability the maximum stress at unloading (σ_{max}) and failure separation distance (δ_f) varies.

(iii) The separation distance at onset of unloading (δ_c) determines the amount of ductile damage before cleavage failure.

A schematic of the proposed unified traction separation law is shown in Figure 1.

Figure 1: Schematic of unified traction separation law.

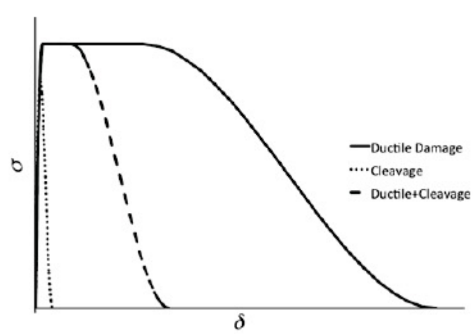

The traction separation law for cleavage failure follows a similar law as shown in Eq. 1 but without the hold at σ_0 and is given by

$$\sigma=\sigma_{max}\begin{cases} 2\left(\dfrac{\delta}{\delta_c}\right)-\left(\dfrac{\delta}{\delta_c}\right)^2, \text{ when } 0<\delta<\delta_c \\ 2\left(\dfrac{\delta-\delta_c}{\delta_f-\delta_c}\right)^3-3\left(\dfrac{\delta-\delta_c}{\delta_f-\delta_c}\right)^2+1, \text{ when } \delta_c<\delta<\delta_f \end{cases} \quad (2)$$

where σ_{max} is the maximum stress ($\sigma_{max} < \sigma_0$) and δ_c, δ_f are the separation distances at onset of damage (unloading) and final failure respectively. In order to improve the stability of FE simulation using cohesive zone model, particularly due to cleavage failure, an artificial viscosity term has been added to the basic traction separation law following (Gao, 2004) as

$$\tilde{\sigma}(\delta)=\sigma(\delta)+\left\langle sign(\delta_f-\delta)\right\rangle \xi \frac{d}{dt}\left(\frac{\delta}{\delta_c}\right) \quad (3)$$

where ξ is the viscosity parameter. In (Gao, 2004), an exponential cohesive law (Xu, 1994) with elastic response for bulk material has been used to describe the methodology. In the present work, the formulation has been extended to Eq.

1 and Eq. 2 with Von Mises plasticity for bulk material. Since the viscosity term adds artificial dissipation to improve convergence behavior under unstable crack growth, it can affect the global response significantly. A parametric study has been performed to estimate the sensitivity of global force-displacement to viscosity parameter. A 1T-CT specimen with an initial crack length of 26.1 mm is considered. The cohesive parameters considered are δ_c = 0.0001 mm, δ_f = 0.0005 mm and σ_{max} = 1810 MPa. Five different viscosity parameters are used and the corresponding modified traction-separation behavior for $d\delta/dt$ = 0.001 mm/s and Δt=0.001s is shown in Figure 2(a). The corresponding force-CMOD is shown in Figure 2(b). The simulation didn't converge without viscosity (ξ = 0).
As can be observed from the figures, the global load-CMOD and predicted fracture toughness have a strong dependence on the viscosity parameter. A higher value of viscosity parameter though allows larger time steps, over estimates the fracture toughness significantly. Hence a viscosity parameter ξ=1 has been considered in the present work.

Figure 2: A study of the effect of viscosity: (a) Traction-separation law (b) Load-CMOD (crack mouth opening displacement).

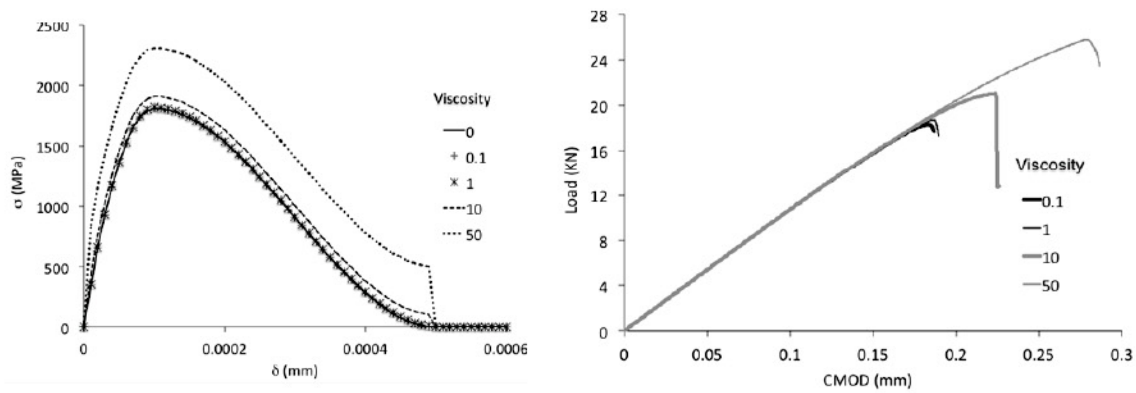

(a) (b)

Unit cell analysis and evaluation of cohesive zone parameters

The cohesive zone parameters for ductile-damage are obtained from plane strain unit cell analysis with the material behavior captured using rate dependent Gurson model. Enhancements proposed in (Tvergaard, 1984) incorporating void nucleation and accelerated void coalescence is considered. In the rate dependent Gurson model, the plastic component of rate of deformation tensor is obtained from

$$\underline{D}^p = \dot{\lambda}\frac{\partial \phi}{\partial \underline{\sigma}} \qquad (4)$$

where the flow potential ϕ is represented by

$$\phi = \frac{\sigma_e^2}{\sigma_m^2} + 2f^* q_1 \cosh\left(\frac{q_2\sigma_h}{2\sigma_m}\right) - 1 - q_3 f^{*2} \qquad (5)$$

and the flow rate $\dot{\lambda}$ is obtained from equivalence of plastic power as

$$\dot{\lambda} = \frac{(1-f)\sigma_m\dot{\varepsilon}_m}{\underline{\sigma}:\partial\phi/\partial\underline{\sigma}} \qquad (6)$$

In Eq. 4, 5 and 6, σ_e is the Von Mises stress, σ_h is the hydrostatic stress, σ_m is the stress in the matrix, ε_m is the viscoplastic strain in the matrix, f* is the modified void volume fraction and q_1, q_2, q_3 are parameters. The viscoplastic strain in the matrix is evolved using a power law as

$$\dot{\varepsilon}_m = \varepsilon_o \left(\frac{\sigma_e}{\sigma_m} \right)^{\frac{1}{m}} \qquad (7)$$

where ε_0 is the reference strain rate and m is the flow exponent. The evolution of void is governed by

$$\dot{f} = \dot{f}_g + \dot{f}_n \qquad (8)$$

where void growth rate $\dot{f}_g$ is defined by

$$\dot{f}_g = (1-f)tr(\underline{D}^p) \qquad (9)$$

and a strain controlled void nucleation rate $\dot{f}_n$ is defined by

$$\dot{f}_n = \frac{f_N}{s_N\sqrt{2\pi}} \exp\left(-\frac{1}{2}\left(\frac{\varepsilon_m - \varepsilon_N}{s_N} \right)^2 \right) \dot{\varepsilon}_m \qquad (10)$$

where f_N, $\square_N$ and ε_N are parameters. Accelerated coalescence of void after a critical void volume fraction is modeled using

$$f^* = \begin{cases} f, \text{ for } f \le f_c \\ f_c + \dfrac{f_u - f_c}{f_f - f_c}, \text{ for } f > f_c \end{cases} \qquad (11)$$

where $f_u=1/q_1$ and f_c and f_f are critical and final void volume fractions respectively.

For the unit cell analysis, a crack tip triaxiality of 3 is assumed and the stress ratio $\beta=\sigma_{11}/\sigma_{22}$ is evaluated from

$$\beta = \frac{\sqrt{3}H - 1}{\sqrt{3}H + 1} \qquad (12)$$

where H is the triaxiality. Two spring elements with constraints are attached at one corner of the unit cell to maintain a fixed stress ratio. A very low strain rate of 0.001 /s has been used to simulate quasi-static behavior.

The room temperature (T=20°C) data reported in (Samal, 2008) has been considered to obtain the Gurson parameters and corresponding traction-separation law for ductile damage. The material parameters are listed below.

(i) Elastic properties [12]:
   E=210 GPa, ν=0.3

(ii) Void parameters [12]:
   f_0=0.0003, f_c=0.05, f_f=0.3

(iii) Void nucleation parameters [20]:
   f_N= 0.04, s_N = 0.1, $\square_N$ = 0.3

(iv) Flow potential parameters [20]:
   q_1=1.5, q_2=1, $q_3=q_1^2$

(v) Viscoplastic parameters
   m=0.005, ε_0=0.0001/s

A very low value of m has been considered to simulate rate independent behavior.

From the unit-cell analysis the σ□ε response along the primary loading direction (22) is obtained. The response is fitted with Eq. 1 and is shown in Figure 3.

The following parameters for the traction separation law are obtained:

(i) Maximum stress σ_0=1869 MPa

(ii) Normalized separation distances δ_e/h=0.005, δ_c/h=0.04, δ_f/h=0.346.

To use the non-dimensional traction separation law parameters in FE simulations, a cell height h needs to be prescribed. Following (Anvari, 2006), h=0.1 mm has been considered which is based on mean inter particulate distance. Plane strain simulation is performed for a 1T-CT specimen with an initial crack length a_0 = 26.1 mm and width W=50 mm to verify the cohesive zone parameters for ductile damage. The FE mesh of the CT specimen is shown in Figure 4. A mesh dimension of 0.02 mm X 0.02 mm different from the cell height is considered at the crack tip. The Load-CMOD (crack mouth opening displacement) and J-resistances are compared with (Samal, 2008) and are shown in 5(a) and 5(b) respectively. The J-resistance curve is obtained following ASTM E1152 (Anderson, 1994). As can observed from the Figures, the correlation with experiments is quite satisfactory.

Figure 3: σ-ε evolution along primary loading direction (22) obtained from unit cell analysis using rate dependent Gurson model and corresponding traction separation law at T=20°C.

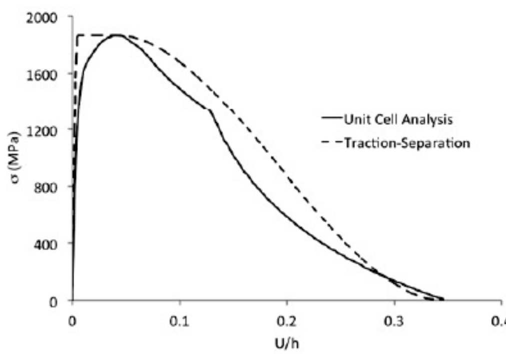

Figure 4: FE mesh of the 1T-CT specimen.

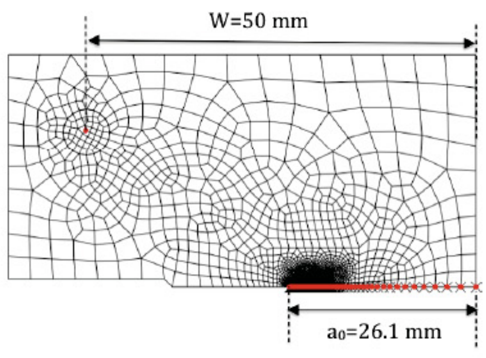

Figure 5: Comparison with experiment at T=20°C: (a) Load-CMOD (b) J-resistance.

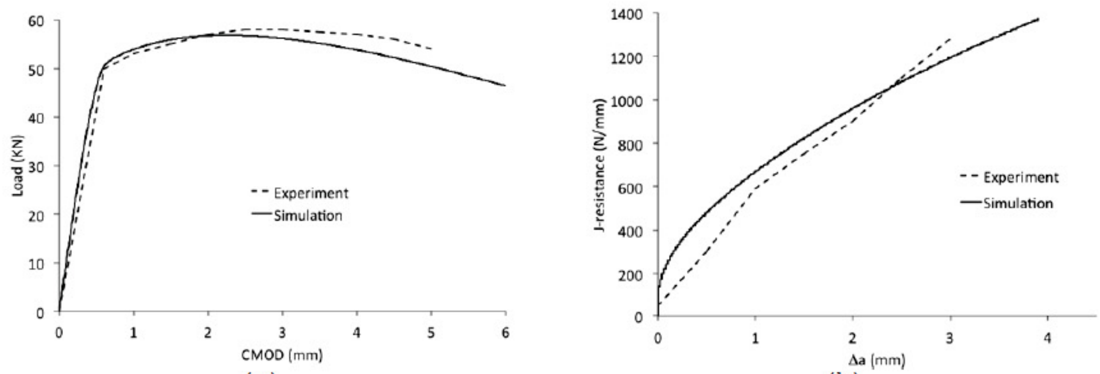

(a) (b)

Unified cohesive law parameters and comparison with master curve

To obtain the parameters of the unified cohesive law, the flow and fracture test results at T=-100°C (Samal, 2008) are considered for calibration. Unit cell analysis with the rate dependent Gurson model parameters described in previous section but a different flow stress behavior is used (Samal, 2008). The non-dimensional traction separation law is shown in Figure 6.

Figure 6: σ-ε evolution along primary loading direction (22) obtained from unit cell analysis using rate dependent Gurson model and corresponding traction separation law at T=-100°C.

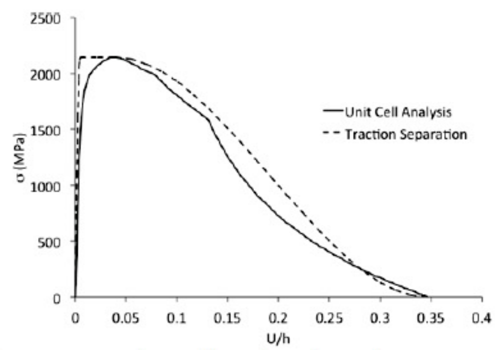

At T=-100°C, failure happens primarily due to cleavage with very little stable crack growth. Hence Eq. 2 is used as the traction separation law with maximum stress σ_{max} corresponding to critical Weibull stresses reported in (Samal, 2008). These are 1840 MPa and 2069 MPa corresponding to 5% and 95% failure probabilities respectively. The critical separation distance δ_c for 5% and 95% failure probabilities is obtained from the ductile damage traction-separation law using

$$\delta_c : \sigma_0 \left(2\left(\frac{\delta_c}{\delta_e}\right) - \left(\frac{\delta_c}{\delta_e}\right)^2 \right) = \sigma_{\max} \qquad (13)$$

and are 0.00015 and 0.0002 mm respectively. The separation distance at final failure δ_f is obtained from a sensitivity study and comparison with experimentally obtained fracture toughness (Samal, 2008). The traction separation law and Load-CMOD for 5% and 95% failure probabilities are shown in Figure 7(a) and 7(b) respectively. Comparison of fracture toughness with Master Curve is shown in Figure 8. As can be observed from Figure 8, $\delta_f = 3\delta_c$ provides reasonable estimate of fracture toughness.

Figure 7: Unified cohesive zone model at T=-100°C: (a) Traction separation law (b) Load-CMOD.

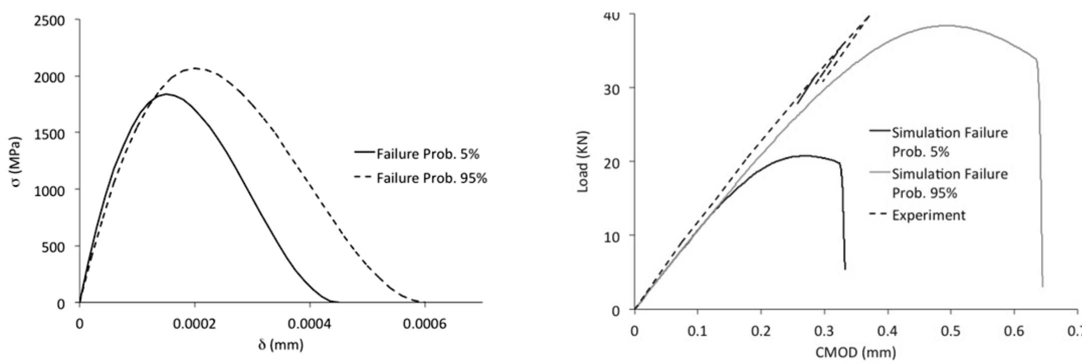

(a) (b)

In (Tanguy, 2005) and (Samal, 2008) the Weibull parameters calibrated at -100°C are used at other temperatures to predict DBT. For the unified cohesive zone law, a similar assumption is made and the maximum stress σ_{max} is held fixed for respective failure probabilities at all other temperatures. The critical separation distance δ_c is evaluated from corresponding ductile damage traction separation law and separation distance at final failure from $\delta_f = 3\delta_c$. As a test case, T=-20°C is considered in the present work. For the 5% probability case, cohesive law parameters σ_{max}=1840 MPa, δ_c=0.00018 mm and $\delta_f = 3\delta_c$ is used. The predicted fracture toughness is compared with the Master curve and is shown in Figure 8. As can be observed from the comparison, $\delta_f=3\delta_c$ grossly underestimates the fracture toughness. This is due to higher levels of plastic deformation at higher temperatures for the same maximum failure stress and hence larger value of δ_f needs to be considered. A final separation distance δ_f=0.001 mm provides reasonably good match as can be seen from Figure 8. For failure probability of 95% at T=-20°C σ_{max} =2069 MPa exceeds for σ_0 for ductile damage (σ_0=2001 MPa). Under such situation Eq. 1 is used as the traction separation law. Values of δ_c=0.001 mm and δ_f=0.0016 mm provides reasonable match with the Master Curve and is shown Figure 8.

Figure 8: Comparison of fracture toughness between unified cohesive law and master curve

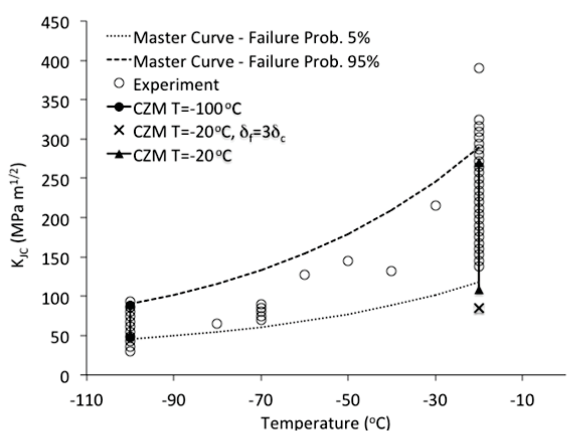

Work is in progress to obtain a correlation for δ_c and δ_f with flow parameters and cohesive zone parameters at T=-100°C.

Conclusions and future work

A unified cohesive zone model has been proposed in the present study to model DBT of RPV steel. In this method both the ductile and cleavage mode of crack growth is modeled as opposed to existing methodologies where stable crack growth through ductile damage is only modeled and initiation of unstable cleavage failure is predicted using a probabilistic model as post-processing after the simulations. The current unified approach avoids the post-processing after the simulations. In the model, it is assumed that the traction separation law follows ductile damage till the onset of unloading due to cleavage. The traction separation parameters for ductile damage for different temperatures were obtained from unit cell analysis. A viscosity term has been added to the traction separation law to improve its stability. The cohesive zone parameters for cleavage failure were calibrated from experiments at T=-100°C. The extensibility of these parameters for other temperatures have been shown by comparing the predictions with experiments at T=-20°C.
An improved correlation between the critical separation distances and temperature needs to be further developed and is in progress. Presently the cohesive law parameters are calibrated from experimentally obtained fracture toughness data, however, more physical lower length scale models can be used to derive the cohesive law parameters.

Acknowledgements

This work was supported by Life Extension of LWRs program at INL.

References

[1] J. F. Knott (1977), "Micromechanisms of fracture and the fracture toughness of engineering alloys," *Fracture*,1, pp. 61-91.

[2] C. J. Jr. McMahon and M. Cohen (1965), "Initiation of cleavage in polycrystalline iron," *Acta. Metal.*,13, pp. 591-604.

[3] E. Smith (1966), "The nucleation and growth of cleavage microcracks in mild steel," in *Proceedings of the Conference on the Physical Basis of Yield and Fracture*, London, pp. 36-46.

[4] R. O. Ritchie, J. F. Knott, and J. R. Rice (1973), "On the relationship between critical tensile stress and fracture toughness in mild steel," *J. Mech. Phys. Solids*,21, pp. 395-410.

[5] D. A. Curry and J. F. Knott (1979), "Effect of microstructure on cleavage fracture toughness in mild steel," *Metal Science*,13, pp. 341-345.

[6] F. M. Beremin (1983), "A local criterion for cleavage fracture of a nuclear pressure vessel steel," *Met. Trans. A*,14A, pp. 2277-2287.

[7] W. Weibull (1953), "A statistical distribution function of wide applicability," *Jour. App. Mech.*,18, pp. 293-297.

[8] G. Rousselier (1987), "Ductile fracture models and their potential in local approach of fracture," *Nuc. Engg. Des.*,105, pp. 97-111.

[9] A. L. Gurson (1977), "Continuum theory of ductile rupture by void nucleation and growth: Part I—yield criteria and flow rules for porous ductile media," *Trans. ASME, Jour. Engg. Mat.*,99, pp. 2-15,.

[10] B. Tanguy, J. Besson, R. Piques, and A. Pineau (2005), "Ductile to brittle transition of an A508 steel characterized by Charpy impact test. Part I: experimental results," *Engg, Frac. Mech.*,72, pp. 49-72.

[11] B. Tanguy, J. Besson, R. Piques, and A. Pineau (2005), "Ductile to brittle transition of an A508 steel characterized by Charpy impact test. Part II: modeling of the Charpy transition curve," *Engg. Frac. Mech.*,72, pp. 413-434.

[12] M. K. Samal, M. Seidenfuss, E. Roos, B. K. Dutta, and H. S. Kushwaha (2008), "Experimental and numerical investigation of ductile-to-brittle transition in a pressure vessel steel," *Mat. Sc. Engg. A*,496, pp.

25-35.

[13] M. K. Samal, M. Seidenfuss, E. Roos, B. K., Dutta, and H. S. Kushwaha (2008), "Finite element formulation of a new nonlocal damage model," *Finite Elem. Ana. Des.*,44, pp. 358-371.

[14] B. Z. Margolin, V. A. Shvetsova, A. G. Gulenko, and V. I. Kostylev (2006), "Application of a new cleavage fracture criterion for fracture toughness prediction for RPV steels," *Fatigue Fract. Engg. Mat. Struct.*,29, pp. 697-713.

[15] L. Vincent, M. Libert, B. Marini, and C. Rey (2010), "Towards a modelling of RPV steel brittle fracture using crystal plasticity computations on polycrystalline aggregates," *Jour. Nuc. Mat.*, 406, pp. 91-96.

[16] I. Scheider and W. Brocks (2003), "Simulation of cup-cone fracture using the cohesive model," *Engg. Frac. Mech.*,70, pp. 1943-61.

[17] V. Tvergaard and J. W. Hutchinson (1992), "The relation between crack growth resitance and fracture process parameters in elastic-plastic solids," *J. Mech. Phys. Solids*,40, pp. 1377-1397,.

[18] Y. F. Gao and A. F. Bower (2004), "A simple technique for avoiding convergence problems in finite element simulations of crack nucleation and growth on cohesive interfaces," *Modelling Simul. Mat. Sci. Engg.*,12, pp. 453-463.

[19] X. P. Xu and A. Needleman (1994), "Numerical simulation of fast crack growth in brittle solids," *J. Mech. Phys. Solids*,42, pp. 1397-1434.

[20] V. Tvergaard and A. Needleman (1984), "Analysis of the cup-cone fracture in a round tensile bar," *Acta. metall.*,32(1), pp. 157-169.

[21] M. Anvari, I. Scheider, and C. Thaulow (2006), "Simulation of dynamic ductile crack growth using strain rate and triaxiality-dependent cohesive elements," *Engg. Frac. Mech.*,73, pp. 2210-2228.

[22] T. L. Anderson (1994), *Fracture Mechanics*, 2nd ed. New York, USA: CRC Press.